



Full length article

On effective surface elastic moduli for microstructured strongly anisotropic coatings

Victor A. Eremeyev^{a,b}, Giuseppe Rosi^{c,*}, Salah Naili^c^a Department of Civil and Environmental Engineering and Architecture (DICAAR), University of Cagliari, Via Marengo, 2, 09123 Cagliari, Italy^b Gdańsk University of Technology, ul. Gabriela Narutowicza 11/12, 80-233 Gdańsk, Poland^c Univ Paris Est Creteil, Univ Gustave Eiffel, CNRS, UMR 8208, MSME, F-94010 Créteil, France

ARTICLE INFO

Keywords:

Surface elasticity
 Effective properties
 Dispersion relation
 Anti-plane waves
 Hyperbolic metasurface

ABSTRACT

The determination of surface elastic moduli is discussed in the context of a recently proposed strongly anisotropic surface elasticity model. The aim of the model was to describe deformations of solids with thin elastic coatings associated with so-called hyperbolic metasurfaces. These metasurfaces can exhibit a quite unusual behaviour and concurrently a very promising wave propagation behaviour. In the model of strongly anisotropic surface elasticity, strain energy as a function of the first and second deformation gradients has been introduced in addition to the constitutive relations in the bulk. In order to obtain values of surface elastic moduli, we compare dispersion relations for anti-plane surface waves obtained using the two-dimensional (2D) model and three-dimensional (3D) straightforward calculations for microstructured coatings of finite thickness. We show that with derived effective surface moduli, the 2D model can correctly describe the wave propagation.

1. Introduction

Nowadays various models of surface elasticity found wide applications in modelling and design of nanostructured materials, see, e.g., (Duan, Wang, & Karihaloo, 2008; Eremeyev, 2016; Heyden & Bain, 2024; Javili, dell'Isola, & Steinmann, 2013; Javili, McBride, & Steinmann, 2013; Wang et al., 2011). In the framework of the surface elasticity concept one introduces a surface strain energy which can be treated as a certain extension of the surface tension notion (Adamson & Gast, 1997). The most popular models of surface elasticity were introduced by Gurtin and Murdoch (1975, 1978) and by Steigmann and Ogden (1997, 1999). This additional surface constitutive relation is independent on the constitutive equations in the bulk, in general. As a result, we have additional material parameters which should be somehow determined. For example, in the case of the linearised Gurtin–Murdoch surface elasticity with isotropic properties we have three additional parameters which are the two surface Lamé moduli λ_s and μ_s and initial surface tension γ , see Duan et al. (2008), Ru (2010) for discussion on possible models. For linearised Steigmann–Ogden model in addition to aforementioned parameters we have two elastic moduli related to bending stiffness, see, e.g., Dai and Schiavone (2023), Han, Mogilevskaya, and Schillingner (2018), Wang, Yan, et al. (2019), Zemlyanova and Mogilevskaya (2018). Obviously, further extensions of surface elasticity require even more material parameters.

Let us note that straightforward experimental measurements of surface elastic *moduli* require rather advanced techniques together with proper models such as atom-force microscopy (Cuenot, Frétygny, Demoustier-Champagne, & Nysten, 2004; Jing et al., 2006; Xu, Jensen, Boltyskiy, Sarfati, Style et al., 2017) or other techniques (Cornelius & Thomas, 2018) which can be applied to specimens at small scales, so such measurements are quite rare. Another source of material parameters is atomistic models and corresponding

* Corresponding author.

E-mail addresses: eremeyev.victor@gmail.com (V.A. Eremeyev), giuseppe.rosi@u-pec.fr (G. Rosi), naili@u-pec.fr (S. Naili).

simulations, see, e.g., Miller and Shenoy (2000), Pourkermani, Azizi, and Pishkenari (2020), Shenoy (2005), Wang, Bian, and Wang (2019). For example, the relations between linear Gurtin–Murdoch model and lattice dynamics can be established if one choose proper scaling (Eremeyev & Sharma, 2019; Sharma & Eremeyev, 2019). It is worth to mention also some other techniques resulting to 2D surface/interface models of thin coatings and interfacial layers (Benveniste & Miloh, 2001, 2007; Brun, Movchan, & Movchan, 2010; Gei, 2008; Kaur, Khurana, & Tomar, 2024; Mishuris, Movchan, & Movchan, 2006, 2010; Mishuris, Öchsner, & Kuhn, 2006; Movchan & Movchan, 1995; Nobili & Volpini, 2021; Sonato, Piccolroaz, Miszuris, & Mishuris, 2015). Some of these techniques are closely related to the surface elasticity, see the discussion in Eremeyev, Rosi, and Naili (2020).

Summarising, we underline that the problem of experimental and/or theoretical determination of a surface elastic parameters is quite complex even in the case of infinitesimal deformations of isotropic solids. At the same time, surface moduli may change significantly effective properties of materials (Duan et al., 2008; Eremeyev, 2016; Han et al., 2018; Wang et al., 2011; Wang & Schiavone, 2013; Wang, Yan, et al., 2019; Zemlyanova & Mogilevskaya, 2018) and affect stress singularity in vicinity of crack tips, see e.g. the discussion in Gorbushin, Eremeyev, and Mishuris (2020). Moreover, surface elasticity essentially enriched a picture of surface waves, see Eremeyev (2024), Eremeyev, Rosi, and Naili (2016), Eremeyev et al. (2020), Jia, Zhang, Zhang, Feng, and Gu (2018), Mikhasev, Botogova, and Eremeyev (2021, 2022), Mikhasev, Erbaş, and Eremeyev (2023), Rosi, Placidi, Nguyen, and Naili (2017), Steigmann and Ogden (2007) and the references therein. The problem becomes more complex for thin microstructured anisotropic coatings such ones used for manufacturing of metasurfaces of different kind. In fact, such coatings as self-cleaned and super oleo- and hydrophobic surfaces have rather complicated microstructure (Bhushan, Jung, & Koch, 2009; Chen, Taylor, & Yu, 2016; Holloway, Kuester, Gordon, O'Hara, Booth et al., 2012). Considering microstructured thin coatings one can use a boundary homogenisation technique similar to homogenisation in 3D. In other words, one can replace a thin surface/interface layer of finite thickness by 2D constitutive equations of the surface elasticity. Some examples of such a technique can be found in Eremeyev (2016), where the Gurtin–Murdoch model was used as the effective medium. Boundary homogenisation techniques have also been shown to be effective in capturing such complex behaviour in other cases, see Bernoff, Lindsay, and Schmidt (2018), Grebenkov and Skvortsov (2023), Plunkett and Lawley (2024).

Motivated by hyperbolic metasurfaces the model of strongly anisotropic surface elasticity was proposed recently in Eremeyev (2019). A hyperbolic metasurface can be considered as a coating made of array of ordered parallel to each other ribs (nanobars) attached to a solid surface (High et al., 2015; Ji et al., 2014; Li et al., 2018; Schwan & Boutin, 2013). From the physical point of view the model (Eremeyev, 2019) describes finite deformations of an elastic solid body with attached on its surface an elastic membrane reinforced by elastic beams. As a result, the introduced surface strain energy inherits bending stiffness of the beams elastic stiffness of the membrane, so it takes into account stretching and bending. But the latter relates to bending along beams. For small deformations we have four elastic moduli. Analysing the anti-plane surface waves with this model we derived specific dispersion relations which are highly sensitive to values of elastic moduli. Let us note that the model (Eremeyev, 2019) was introduced within so-called direct approach. In fact, motivated by observed microstructure of hyperbolic metasurfaces the form of the surface strain energy was postulated as a constitutive relation for 2D elastic continuum.

The aim of this paper is discuss the behaviour of solids with microstructured coatings of finite thickness similar to reinforced elastic membranes and to determine their effective elastic properties. The paper is organised as follows. First, following (Eremeyev, 2019) we briefly recall the basic equations of the strongly anisotropic elasticity in Section 2. For simplicity we restrict ourselves by infinitesimal deformations. In Section 3 we consider anti-plane deformations. In Section 4 we introduce the corresponding 3D model of a coating of finite thickness and describe the calculation technique. Here we analyse the dispersion relations for both models. Comparing these relations we obtain the effective elastic surface moduli.

2. Basic equations of the strongly anisotropic surface elasticity

Following (Eremeyev, 2019), let us briefly recall the basic equations of the model, derived using variational modelling based on the least action principle (Eremeyev, 2019). This means that the equations of motion and boundary conditions are obtained from the minimisation of the action functional, *i.e.* the integral of the difference between the kinetic energy and potential energy. As was mentioned in Introduction, the strongly anisotropic surface elasticity was motivated by some metasurfaces. Schematic representation of a solid body with such a surface is given in Fig. 1. It consists of a system of almost parallel interacting ribs (fibres). From the mechanical point of view, the solid could be treated as a system of elastic beams connected *via* elastic bonds modelled as elastic springs. Obviously, there is a preferable direction along beams which can be parameterised using a surface unit vector $\underline{\tau}$ with $\underline{\tau} \cdot \underline{n} = 0$, where \underline{n} is a normal unit vector to the surface. Such a coating could be treated as an elastic membrane reinforced by elastic fibres. This membrane has no bending stiffness related to the bending in the plane orthogonal to $\underline{\tau}$.

For simplicity we restrict ourselves by infinitesimal deformations of an isotropic in the bulk elastic solid. So the kinematics is described through a displacement vector field given by

$$\underline{u} = \underline{u}(\underline{x}, t), \quad (1)$$

where \underline{x} is the position vector and t is time. In the bulk, we have the Hooke law and the second-order tensor of infinitesimal strains defined by

$$\underline{\underline{\sigma}} = \lambda (\text{Tr } \underline{\underline{e}}) \underline{\underline{I}} + 2\mu \underline{\underline{e}}, \quad \underline{\underline{e}} = \frac{1}{2} (\nabla \underline{u} + (\nabla \underline{u})^T), \quad (2)$$

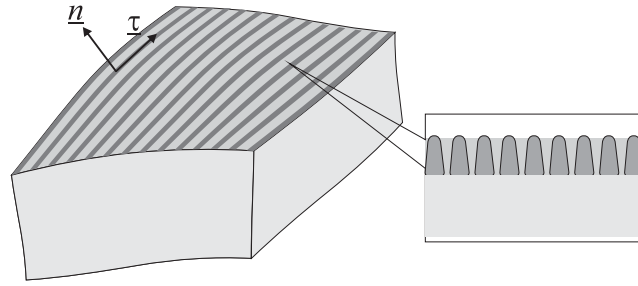


Fig. 1. Illustration of a microstructured coating (metasurface).

where λ and μ are the Lamé moduli, Tr is the trace operator, \underline{I} is the 3D unit second-order tensor, $\underline{\sigma}$ and $\underline{\epsilon}$ are the second-order tensors of stress and strain, respectively. The 3D nabla-operator $\underline{\nabla}$ allows to define the gradient and divergence operators denoted $\underline{\nabla}$ and $\underline{\nabla} \cdot$ respectively. The equation of motion takes the form

$$\mu \underline{\nabla} \cdot \underline{\nabla} \underline{u} + (\lambda + \mu) \underline{\nabla} \underline{\nabla} \cdot \underline{u} = \rho \ddot{\underline{u}}, \tag{3}$$

where ρ is mass density of the solid and the overdot stands for the derivative with respect to t .

In addition to constitutive relations in the bulk, we introduce the surface strain energy density W_s as follows (Eremeyev, 2019)

$$\begin{aligned} W_s = & K_1 \text{Tr}(\underline{\epsilon}^2) + \frac{1}{2} K_2 (\text{Tr} \underline{\epsilon})^2 + \frac{1}{2} K_3 (\underline{\tau} \cdot \underline{\epsilon} \cdot \underline{\tau})^2 + \frac{1}{2} K_4 (\underline{\tau} \cdot \underline{\epsilon} \cdot \underline{\tau})(\text{Tr} \underline{\epsilon}) \\ & + \frac{1}{2} K_b [\underline{\tau} \times (\underline{\tau} \cdot \underline{\nabla}_s)(\underline{\tau} \cdot \underline{\nabla}_s) \underline{u}] \cdot [\underline{\tau} \times (\underline{\tau} \cdot \underline{\nabla}_s)(\underline{\tau} \cdot \underline{\nabla}_s) \underline{u}], \end{aligned} \tag{4}$$

where K_1 and K_2 are the surface Lamé moduli as in the linear Gurtin–Murdoch surface elasticity, K_3 and K_4 relate to fibre reinforcement, K_b is the higher order elastic modulus related to bending stiffness of fibres, and \times is the cross product. In addition, $\underline{\epsilon}$ is the second-order tensor of surface strain given by

$$\underline{\epsilon} = \frac{1}{2} \left(\underline{\nabla}_s \underline{u} \cdot \underline{A} + \underline{A} \cdot (\underline{\nabla}_s \underline{u})^T \right),$$

where $\underline{A} = \underline{I} - \underline{n} \otimes \underline{n}$ is the second-order tensor of perpendicular projection onto the tangent plan to the surface, $\underline{\nabla}_s = \underline{A} \cdot \underline{\nabla}$ is the surface gradient operator, and \otimes is the dyadic product. The first line of Eq. (4) coincides with two-dimensional constitutive relations of fibre reinforced materials, see Smith (1994), Spencer (1984), whereas the last term describes bending energy contribution.

Eq. (4) results in the following surface stresses and hyperstresses respectively:

$$\begin{aligned} \underline{\underline{S}} = \frac{\partial W_s}{\partial \underline{\epsilon}} = & 2K_1 \underline{\epsilon} + \left(K_2 (\text{Tr} \underline{\epsilon}) + K_4 \underline{\tau} \cdot \underline{\epsilon} \cdot \underline{\tau} \right) \underline{A} \\ & + \left(K_3 \underline{\tau} \cdot \underline{\epsilon} \cdot \underline{\tau} + K_4 (\text{Tr} \underline{\epsilon}) \right) \underline{\tau} \otimes \underline{\tau}, \end{aligned} \tag{5}$$

$$\underline{\underline{M}} = \frac{\partial W_s}{\partial \underline{\nabla}_s \underline{\nabla}_s \underline{u}} = K_b \underline{\tau} \otimes \underline{\tau} \otimes \underline{\tau} \otimes \underline{\tau} \otimes \left[(\underline{\tau} \otimes \underline{\tau}) : \underline{\nabla}_s \underline{\nabla}_s \underline{u} \right] \times \underline{\tau}. \tag{6}$$

The corresponding boundary conditions for a smooth surface, they are given by the formula

$$\underline{\sigma} \cdot \underline{n} = \underline{\nabla}_s \cdot \underline{\underline{S}} - \underline{\nabla}_s \cdot (\underline{\nabla}_s \cdot \underline{\underline{M}}) - 2H \underline{n} \cdot (\underline{\nabla}_s \cdot \underline{\underline{M}}) - m \ddot{\underline{x}}, \tag{7}$$

where m is surface mass density and the scalar $H = -1/2 \underline{\nabla}_s \cdot \underline{n}$ is the mean curvature of the surface where the surface stresses act. Eq. (7) plays a role of the generalised Laplace–Young equation. These boundary conditions represent the coupling between the bulk substrate and the coating. The right hand of Eq. (7) is composed by four terms: the first one includes the contribution from membrane-like behaviour (both in shear and traction), the second and third one include the bending-like behaviour induced mainly by the stiff fibres, while the last one is an inertial term.

Note that (4) is an example of so-called surface strain gradient elasticity with a surface strain energy also dependent of gradient of strain:

$$W_s = W_s(\underline{\epsilon}, \underline{\nabla}_s \underline{\nabla}_s \underline{u}). \tag{8}$$

Even more complex cases were discussed in Eremeyev, Lebedev, and Cloud (2021), Rodriguez (2024).

3. Anti-plane motions

The basic equations discussed previously can be significantly simplified in the case of anti-plane deformations. Here, the motions are assumed in the following form (Achenbach, 1973)

$$\underline{u} = u(x_1, x_3, t) \underline{e}_2, \tag{9}$$

where (x_1, x_2, x_3) are Cartesian coordinates in the orthonormal basis $(\underline{e}_1, \underline{e}_2, \underline{e}_3)$. In the following, we consider the half-space $x_3 \leq 0$, so the external normal \underline{n} coincides with \underline{e}_3 whereas $\underline{\tau} = \underline{e}_2$.

Hereinafter, for brevity, we use the following notations for spatial derivatives: $\partial_1 = \partial/\partial x_1$, $\partial_3 = \partial/\partial x_3$. From Eq. (9), we have that

$$\begin{aligned}\nabla \underline{u} &= (\partial_1 u \underline{e}_1 + \partial_3 u \underline{e}_3) \otimes \underline{e}_2, \quad \nabla_s \underline{u} = \partial_1 (u_2 \underline{e}_1 \otimes \underline{e}_2), \\ \nabla_s \nabla_s \underline{u} &= \partial_1^2 u (\underline{e}_1 \otimes \underline{e}_1 \otimes \underline{e}_2), \\ \underline{\underline{\sigma}} &= \mu [\partial_1 u (\underline{e}_1 \otimes \underline{e}_2 + \underline{e}_2 \otimes \underline{e}_1) + \partial_3 u (\underline{e}_2 \otimes \underline{e}_3 + \underline{e}_3 \otimes \underline{e}_2)], \\ \underline{\underline{S}} &= K_1 \partial_1 u (\underline{e}_1 \otimes \underline{e}_2 + \underline{e}_2 \otimes \underline{e}_1), \quad \underline{\underline{M}} = K_b \partial_1^2 u (\underline{e}_1 \otimes \underline{e}_1 \otimes \underline{e}_2).\end{aligned}\quad (10)$$

Using (9) and (10), the equation of motion (3) reduces to the wave equation given by

$$\mu (\partial_1^2 + \partial_3^2) u = \rho \ddot{u}, \quad (11)$$

whereas the boundary conditions (7) take the form (Eremeyev, 2019)

$$\mu \partial_3 u = -m \ddot{u} + K_1 \partial_1^2 u - K_b \partial_1^4 u. \quad (12)$$

Assuming a steady state condition and looking for solution of (11) in the form

$$u = U(x_1, x_3) \exp(i\omega t), \quad (13)$$

where ω is a circular frequency, i is the imaginary unit, and U is an amplitude, we obtain that Eremeyev (2019)

$$U = U_0 \exp(\kappa x_3) \exp(ikx_1), \quad (14)$$

where

$$\kappa = \kappa(k, \omega) \equiv \sqrt{k^2 - \frac{\omega^2}{c_T^2}}, \quad c_T = \sqrt{\frac{\mu}{\rho}},$$

k is a wavenumber, c_T is the phase velocity of transverse waves in the bulk, and U_0 is a constant. Here, k and ω are related to each other through the dispersion relation

$$\mu \kappa(k, \omega) = m \omega^2 - K_1 k^2 + K_b k^4. \quad (15)$$

We transform Eq. (15) into

$$c^2 = c_s^2 + c_b^2 k^2 + \frac{\mu}{m} \frac{1}{|k|} \sqrt{1 - \frac{c^2}{c_T^2}}, \quad (16)$$

where $c_s = \sqrt{K_1/m}$ is the surface shear wave velocity within the Gurtin–Murdoch model (Eremeyev et al., 2016), $c_b = \sqrt{K_b/m}$ is a bending phase velocity coefficient (bending phase velocity is $k c_b$) and $c = \omega/k$ the phase velocity of the surface wave.

4. 3D finite element numerical validation

In order to evaluate the dispersion for surface waves in a material with fibre coating, a 3D numerical calculation using the finite element method has been developed. The geometry is illustrated in Fig. 2. Given the periodicity of the structure, only a representative unit cell is used in the numerical simulations. Bloch–Floquet periodic boundary conditions have been imposed on the lateral boundaries, free conditions on the upper boundary while the lower boundary is fixed.

The stiffer fibres have a width of h_f , a thickness of H_f and are separated by a layer of filling material of with h_s . This means that the width $L = h_f + h_s$ of the unit cell is imposed by the periodicity of the fibre arrangement. As the wave propagates towards direction \underline{e}_1 , the length a is related to the maximum achievable wavenumber, defined as $k_{max} = 2\pi/a$. The thickness H of the substrate is chosen sufficiently large to ensure a proper exponential decay of the solution, which has the form of Eq. (14), thus matching the fixed boundary condition. The problem is solved using the commercial software Comsol Multiphysics. A wavenumber k_i with $i \in [1, N_p]$ is imposed and the eigenfrequencies of the system are calculated, where N_p is positive integer. Among all the computed modes, anti-plane surface modes are selected by taking into only the eigenvectors in the form of Eq. (14) and the corresponding frequency is noted ω_i . Finally, the phase velocity of the surface wave is computed considering that

$$c_{FEM}(k_i) = \frac{\omega_i}{k_i}.$$

In terms of material properties, three different materials are used (see Table 1):

The geometric features of the solid are $h_f = 50 \mu\text{m}$, $h_s = 50 \mu\text{m}$, $a = 25 \mu\text{m}$. The phase velocity of shear waves in the substrate is $c_T = 3121.95 \text{ m/s}$. For the considered geometry features and material properties, the surface mass density m can be computed as

$$m = \frac{\rho_1 h_f + \rho_2 h_s}{h_f + h_s} H_f.$$

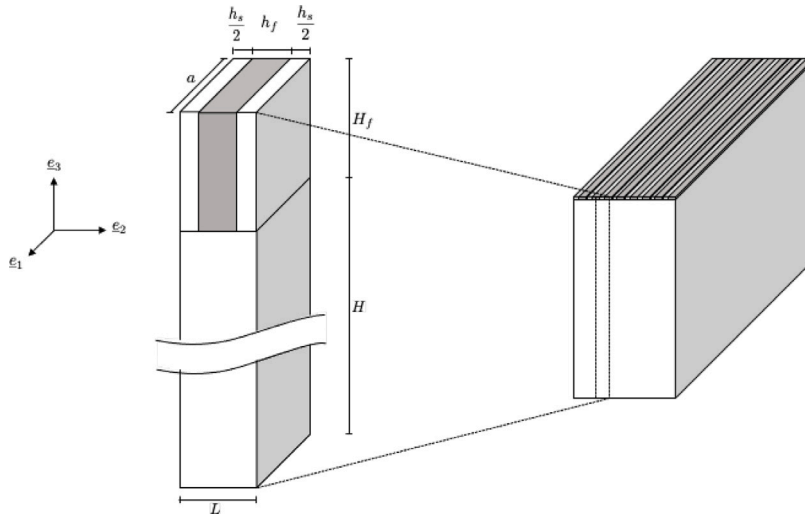


Fig. 2. Illustration of the 3D model.

Table 1

Material properties of the considered coated half-space for $j = 1, 3$.

Material	Young's modulus (E_j [GPa])	Poisson's ratio (ν_j [-])	Mass density (ρ_j [kg/m ³])
Fibre (Material 1)	105	0.33	4900
Filling (Material 2)	50	0.3	2000
Substrate (Material 3)	70	0.33	2700

Table 2

Material properties of the surface elasticity model.

H_f [μm]	m [kg/m ²]	K_b [Pa m ⁴]	K_1 [MPa m]	c_b [m ² /s]	c_s [m/s]
50	0.175	3.679×10^{-6}	1.273	4.618×10^{-3}	2716.44
100	0.345	12.14×10^{-6}	2.522	5.931×10^{-3}	2703.75
300	1.035	46.34×10^{-6}	7.593	6.691×10^{-3}	2708.61
500	1.725	76.56×10^{-6}	12.73	6.662×10^{-3}	2716.23

The other parameters of the surface model have been computed by solving the following minimisation problem:

$$(c_s, c_b) = \arg \min_{c_s, c_b} f(c_s, c_b) = \arg \min_{c_s, c_b} \sum_{i=1}^{N_p} (c(k_i) - c_{FEM}(k_i))^2,$$

where $\arg \min$ is defined as the set of values of $\{c_s, c_b\}$ for which the minimum of $f(c_s, c_b)$ is attained.

In order to test the robustness of the model, a parametric study with respect to the thickness H_f has been performed, and the minimisation procedure leads to the following parameters for the surface model (see Table 2):

In Fig. 3, the results for phase velocity are presented. The markers are related to the numerical solution, the solid line corresponds to the solutions computed with the proposed surface model, while the dashed lines correspond to the classic Gurtin–Murdoch model. It can be remarked that the proposed model fits very well the numerical solution for all the considered values of H_f , and as expected, the model is slightly less accurate when the thickness of the coating increases.

For each value of H_f , the solutions share the same behaviour. For low values of the wavenumber, phase velocity tends to c_T , i.e. phase velocity in the bulk material of the half-space. As expected, when wavenumber increases, the phase velocity decreases following the solution provided by the Gurtin–Murdoch model. However, instead of converging to the asymptotic value c_s , it starts increasing and tends to the asymptotic value $k c_b$ up to the value c_T , as shown in Eremeyev (2019). This can be explained by the dispersive behaviour of the architected coating that becomes dominant as the penetration of the wave inside the material gets smaller. Indeed, for high values of frequency the waves are almost confined within the coating, and the bending behaviour becomes dominant.

5. Conclusions

We have demonstrated that microstructured coatings of finite thickness can be modelled using properly modified surface elasticity, i.e. replacing 3D surface layer by a material surface. Let us note that for anti-plane motions there is no difference between

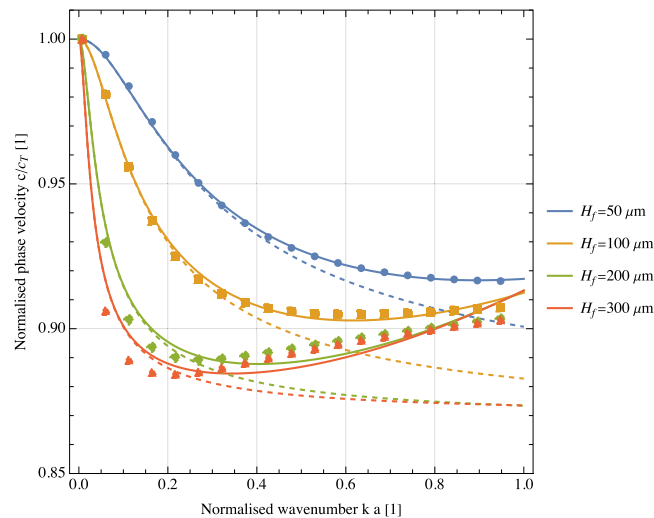


Fig. 3. Normalised phase velocity c/c_T as function of the normalised wavenumber ka .

the Gurtin–Murdoch and Steigmann–Ogden models. When comparing to a FEM simulation (see Fig. 3), these models have been shown to capture correctly the behaviour up to a certain value of the normalised wavenumber. When this value increases, the solution phase velocity of surface waves starts increasing, due to the dispersive behaviour of the coating, while the solution given by Gurtin–Murdoch and Steigmann–Ogden models converges to the value of the shear wave velocity in the bulk. In this regime, the model proposed in Eremeyev (2019), that includes a more general form of constitutive surface strain energy, correctly fits the FEM solution. It is worth to underline that the model (Eremeyev, 2019) includes rather simple form of the surface kinetic energy. In fact, there the rotary inertia or microinertia was not taken into account, see the recent discussion about microinertia by Eremeyev and Elishakoff (2024). Despite of its relative simplicity this 2D model fits quite good the results of exact 3D calculations. To correctly capture wave propagation in a more general context, further studies involving strain gradient surface elasticity with more complex constitutive Eqs. (8) could be necessary.

The obtained values of an surface elastic *moduli* can be also implemented for further modelling within finite element method of solids with surface stresses as in He and Park (2018), Javili and Steinmann (2010), Yvonnet, Quang, and He (2008).

CRedit authorship contribution statement

Victor A. Eremeyev: Writing – review & editing, Writing – original draft, Visualization, Validation, Supervision, Resources, Project administration, Methodology, Investigation, Funding acquisition, Formal analysis, Conceptualization. **Giuseppe Rosi:** Writing – review & editing, Writing – original draft, Visualization, Validation, Software, Methodology, Investigation, Funding acquisition, Formal analysis. **Salah Naili:** Writing – review & editing, Supervision, Project administration, Methodology, Investigation, Funding acquisition, Conceptualization.

Declaration of competing interest

The authors declare the following financial interests/personal relationships which may be considered as potential competing interests: Victor Eremeyev reports financial support was provided by Horizon Europe. Giuseppe Rosi reports financial support was provided by University of Cagliari. Victor Eremeyev reports financial support was provided by Université Paris Est Créteil. Victor Eremeyev reports financial support was provided by Ministero Università e Ricerca. If there are other authors, they declare that they have no known competing financial interests or personal relationships that could have appeared to influence the work reported in this paper.

Data availability

Data will be made available on request.

Acknowledgements

V.A.E. acknowledges the support within the project “Metamaterials design and synthesis with applications to infrastructure engineering” funded by the MUR Progetti di Ricerca di Rilevante Interesse Nazionale (PRIN) Bando 2022 – grant 20228CPHN5, Italy, and the support of the European Union’s Horizon 2020 research and innovation programme under the RISE MSCA EffectFact Project agreement No 101008140. He is also thankful to the Université Paris-Est Créteil Val de Marne (France) and International Research Project (IRP) Coss&Vita from CNRS for the support and hospitality during the visiting professorship programme. G.R. acknowledges the support of the University of Cagliari (Italy) through the visiting professorship program.

References

- Achenbach, J. (1973). *Wave propagation in elastic solids*. Amsterdam: North Holland.
- Adamson, A. W., & Gast, A. P. (1997). *Physical chemistry of surfaces* (6th ed.). New York: Wiley.
- Benveniste, Y., & Miloh, T. (2001). Imperfect soft and stiff interfaces in two-dimensional elasticity. *Mechanics of Materials*, 33(6), 309–323.
- Benveniste, Y., & Miloh, T. (2007). Soft neutral elastic inhomogeneities with membrane-type interface conditions. *Journal of Elasticity*, 88(2), 87–111.
- Bernoff, A. J., Lindsay, A. E., & Schmidt, D. D. (2018). Boundary homogenization and capture time distributions of semipermeable membranes with periodic patterns of reactive sites. *Multiscale Modeling & Simulation*, 16(3), 1411–1447. <http://dx.doi.org/10.1137/17m1162512>.
- Bhushan, B., Jung, Y. C., & Koch, K. (2009). Micro-, nano- and hierarchical structures for superhydrophobicity, self-cleaning and low adhesion. *Philosophical Transactions of the Royal Society A: Mathematical, Physical and Engineering Sciences*, 367(1894), 1631–1672.
- Brun, M., Movchan, A. B., & Movchan, N. V. (2010). Shear polarisation of elastic waves by a structured interface. *Continuum Mechanics and Thermodynamics*, 22(6–8), 663–677.
- Chen, H.-T., Taylor, A. J., & Yu, N. (2016). A review of metasurfaces: Physics and applications. *Reports on Progress in Physics*, 79(7), Article 076401.
- Cornelius, T. W., & Thomas, O. (2018). Progress of in situ synchrotron X-ray diffraction studies on the mechanical behavior of materials at small scales. *Progress in Materials Science*, 94, 384–434.
- Cuenot, S., Fréty, C., Demoustier-Champagne, S., & Nysten, B. (2004). Surface tension effect on the mechanical properties of nanomaterials measured by atomic force microscopy. *Physical Review B*, 69(16), Article 165410.
- Dai, M., & Schiavone, P. (2023). Discussion of the linearized version of the Steigmann-Ogden surface model in plane deformation and its application to inclusion problems. *International Journal of Engineering Science*, 192, Article 103931.
- Duan, H. L., Wang, J., & Karihaloo, B. L. (2008). Theory of elasticity at the nanoscale. In *Adv. appl. mech.*: vol. 42, (pp. 1–68). Elsevier.
- Eremeyev, V. A. (2016). On effective properties of materials at the nano- and microscales considering surface effects. *Acta Mechanica*, 227(1), 29–42.
- Eremeyev, V. A. (2019). Strongly anisotropic surface elasticity and antiplane surface waves. *Philosophical Transactions of the Royal Society of London A (Mathematical and Physical Sciences)*, 378(2162), Article 20190100. <http://dx.doi.org/10.1098/rsta.2019.0100>.
- Eremeyev, V. A. (2024). Surface finite viscoelasticity and surface anti-plane waves. *International Journal of Engineering Science*, 196, Article 104029.
- Eremeyev, V. A., & Elishakoff, I. (2024). On rotary inertia of microstructured beams and variations thereof. *Mechanics Research Communications*, 135, Article 104239.
- Eremeyev, V. A., Lebedev, I. P., & Cloud, M. J. (2021). On weak solutions of boundary value problems within the surface elasticity of N th order. *ZAMM-Journal of Applied Mathematics and Mechanics/Zeitschrift für Angewandte Mathematik und Mechanik*, 101(3), Article e202000378.
- Eremeyev, V. A., Rosi, G., & Naili, S. (2016). Surface/interfacial anti-plane waves in solids with surface energy. *Mechanics Research Communications*, 74, 8–13.
- Eremeyev, V. A., Rosi, G., & Naili, S. (2020). Transverse surface waves on a cylindrical surface with coating. *International Journal of Engineering Science*, 147, Article 103188.
- Eremeyev, V. A., & Sharma, B. L. (2019). Anti-plane surface waves in media with surface structure: Discrete vs. continuum model. *International Journal of Engineering Science*, 143, 33–38.
- Gei, M. (2008). Elastic waves guided by a material interface. *European Journal of Mechanics A - Solids*, 27(3), 328–345.
- Gorbushin, N., Eremeyev, V. A., & Mishuris, G. (2020). On stress singularity near the tip of a crack with surface stresses. *International Journal of Engineering Science*, 146, Article 103183.
- Grebekov, D. S., & Skvortsov, A. T. (2023). Boundary homogenization for target search problems. <http://dx.doi.org/10.48550/arxiv.2310.14322>, arXiv arXiv:2310.14322.
- Gurtin, M. E., & Murdoch, A. I. (1975). A continuum theory of elastic material surfaces. *Archive of Rational Mechanics and Analysis*, 57(4), 291–323.
- Gurtin, M. E., & Murdoch, A. I. (1978). Surface stress in solids. *International Journal of Solids and Structures*, 14(6), 431–440.
- Han, Z., Mogilevskaya, S. G., & Schillinger, D. (2018). Local fields and overall transverse properties of unidirectional composite materials with multiple nanofibers and Steigmann-Ogden interfaces. *International Journal of Solids and Structures*, 147, 166–182.
- He, J., & Park, H. S. (2018). A methodology for modeling surface effects on stiff and soft solids. *Computational Mechanics*, 61(6), 687–697.
- Heyden, S., & Bain, N. (2024). From a distance: Shuttleworth revisited. *Soft Matter*, 20(28), 5592–5597.
- High, A. A., Devlin, R. C., Dibos, A., Polking, M., Wild, D. S., Perczel, J., de Leon, N. P., Lukin, M. D., & Park, H. (2015). Visible-frequency hyperbolic metasurface. *Nature*, 522(7555), 192.
- Holloway, C. L., Kuester, E. F., Gordon, J. A., O'Hara, J., Booth, J., & Smith, D. R. (2012). An overview of the theory and applications of metasurfaces: The two-dimensional equivalents of metamaterials. *IEEE Antennas and Propagation Magazine*, 54(2), 10–35.
- Javili, A., dell'Isola, F., & Steinmann, P. (2013). Geometrically nonlinear higher-gradient elasticity with energetic boundaries. *Journal of Mechanics and Physics of Solids*, 61(12), 2381–2401.
- Javili, A., McBride, A., & Steinmann, P. (2013). Thermomechanics of solids with lower-dimensional energetics: On the importance of surface, interface, and curve structures at the nanoscale. A unifying review. *Applied Mechanics Reviews*, 65(1), Article 010802.
- Javili, A., & Steinmann, P. (2010). A finite element framework for continua with boundary energies. Part II: The three-dimensional case. *Computer Methods in Applied Mechanics and Engineering*, 199(9–12), 755–765.
- Ji, D., Song, H., Zeng, X., Hu, H., Liu, K., Zhang, N., & Gan, Q. (2014). Broadband absorption engineering of hyperbolic metafilm patterns. *Scientific Reports*, 4, 4498.
- Jia, F., Zhang, Z., Zhang, H., Feng, X.-Q., & Gu, B. (2018). Shear horizontal wave dispersion in nanolayers with surface effects and determination of surface elastic constants. *Thin Solid Films*, 645(Supplement C), 134–138.
- Jing, G. Y., Duan, H., Sun, X. M., Zhang, Z. S., Xu, J., Li, Y. D., Wang, J. X., & Yu, D. P. (2006). Surface effects on elastic properties of silver nanowires: Contact atomic-force microscopy. *Physical Review B*, 73(23), Article 235409.
- Kaur, S., Khurana, A., & Tomar, S. (2024). An approximate secular equation of Rayleigh-like waves in coated elastic half-space containing voids. *International Journal of Engineering Science*, 196, Article 104016.

- Li, P., Dolado, I., Alfaro-Mozaz, F. J., Casanova, F., Hueso, L. E., Liu, S., Edgar, J. H., Nikitin, A. Y., Vélez, S., & Hillenbrand, R. (2018). Infrared hyperbolic metasurface based on nanostructured van der Waals materials. *Science*, 359(6378), 892–896.
- Mikhasev, G. I., Botogova, M. G., & Eremeyev, V. A. (2021). On the influence of a surface roughness on propagation of anti-plane short-length localized waves in a medium with surface coating. *International Journal of Engineering Science*, 158, Article 103428.
- Mikhasev, G. I., Botogova, M. G., & Eremeyev, V. A. (2022). Anti-plane waves in an elastic thin strip with surface energy. *Philosophical Transactions of the Royal Society, Series A*, 380(2231), Article 20210373.
- Mikhasev, G., Erbaş, B., & Eremeyev, V. A. (2023). Anti-plane shear waves in an elastic strip rigidly attached to an elastic half-space. *International Journal of Engineering Science*, 184, 103809.
- Miller, R. E., & Shenoy, V. B. (2000). Size-dependent elastic properties of nanosized structural elements. *Nanotechnology*, 11(3), 139–147.
- Mishuris, G. S., Movchan, N. V., & Movchan, A. B. (2006). Steady-state motion of a Mode-III crack on imperfect interfaces. *The Quarterly Journal of Mechanics & Applied Mathematics*, 59(4), 487–516.
- Mishuris, G. S., Movchan, N. V., & Movchan, A. B. (2010). Dynamic mode-III interface crack in a bi-material strip. *International Journal of Fracture*, 166(1–2), 121–133.
- Mishuris, G., Öchsner, A., & Kuhn, G. (2006). FEM-analysis of nonclassical transmission conditions between elastic structures. part 2: Stiff imperfect interface. *CMC: Computers, Materials, & Continua*, 4(3), 137–152.
- Movchan, A. B., & Movchan, N. V. (1995). *Mathematical modelling of solids with nonregular boundaries*. Boca Raton: CRC Press.
- Nobili, A., & Volpini, V. (2021). Microstructured induced band pattern in Love wave propagation for novel nondestructive testing (NDT) procedures. *International Journal of Engineering Science*, 168, Article 103545.
- Plunkett, C. E., & Lawley, S. D. (2024). Boundary homogenization for partially reactive patches. *Multiscale Modeling & Simulation*, 22(2), 784–810. <http://dx.doi.org/10.1137/23m1573422>.
- Pourkermani, A. G., Azizi, B., & Pishkenari, H. N. (2020). Vibrational analysis of Ag, Cu and Ni nanobeams using a hybrid continuum-atomistic model. *International Journal of Mechanical Sciences*, 165, Article 105208.
- Rodríguez, C. (2024). Elastic solids with strain-gradient elastic boundary surfaces. *Journal of Elasticity*, 1–29.
- Rosi, G., Placidi, L., Nguyen, V.-H., & Naili, S. (2017). Wave propagation across a finite heterogeneous interphase modeled as an interface with material properties. *Mechanics Research Communications*, 84, 43–48.
- Ru, C. Q. (2010). Simple geometrical explanation of Gurtin-Murdoch model of surface elasticity with clarification of its related versions. *Science China Physics, Mechanics and Astronomy*, 53(3), 536–544.
- Schwan, L., & Boutin, C. (2013). Unconventional wave reflection due to "resonant surface". *Wave Motion*, 50(4), 852–868.
- Sharma, B. L., & Eremeyev, V. A. (2019). Wave transmission across surface interfaces in lattice structures. *International Journal of Engineering Science*, 145, Article 103173.
- Shenoy, V. B. (2005). Atomistic calculations of elastic properties of metallic fcc crystal surfaces. *Physical Review B*, 71(9), Article 094104.
- Smith, G. F. (1994). *Constitutive equations for anisotropic and isotropic materials*. Amsterdam, New York: North-Holland, Elsevier.
- Sonato, M., Piccolroaz, A., Miszuris, W., & Mishuris, G. (2015). General transmission conditions for thin elasto-plastic pressure-dependent interphase between dissimilar materials. *International Journal of Solids and Structures*, 64, 9–21.
- Spencer, A. J. M. (Ed.), (1984). *Continuum theory of the mechanics of fibre-reinforced composites*. In *CISM courses and lectures: vol. 282*, Wien: Springer.
- Steigmann, D. J., & Ogden, R. W. (1997). Plane deformations of elastic solids with intrinsic boundary elasticity. *Proceedings of the Royal Society A*, 453(1959), 853–877.
- Steigmann, D. J., & Ogden, R. W. (1999). Elastic surface-substrate interactions. *Proceedings of the Royal Society A*, 455(1982), 437–474.
- Steigmann, D. J., & Ogden, R. W. (2007). Surface waves supported by thin-film/substrate interactions. *IMA Journal of Applied Mathematics*, 72(6), 730–747.
- Wang, J., Bian, J., & Wang, G. (2019). Calculation of surface energy density of rough surface by atomic simulations. *Applied Surface Science*, 484, 184–188.
- Wang, J., Huang, Z., Duan, H., Yu, S., Feng, X., Wang, G., Zhang, W., & Wang, T. (2011). Surface stress effect in mechanics of nanostructured materials. *Acta Mechica Solida Sinica*, 24, 52–82.
- Wang, X., & Schiavone, P. (2013). Surface effects in the deformation of an anisotropic elastic material with nano-sized elliptical hole. *Mechanics Research Communications*, 52, 57–61.
- Wang, J., Yan, P., Dong, L., & Atluri, S. N. (2019). Eshelby tensors and overall properties of nano-composites considering both interface stretching and bending effects. *International Journal of Solids and Structures*, in press.
- Xu, Q., Jensen, K. E., Boltyskiy, R., Sarfati, R., Style, R. W., & Dufresne, E. R. (2017). Direct measurement of strain-dependent solid surface stress. *Nature Communications*, 8(1), 555.
- Yvonnet, J., Quang, H. L., & He, Q.-C. (2008). An XFEM/level set approach to modelling surface/interface effects and to computing the size-dependent effective properties of nanocomposites. *Computational Mechanics*, 42(1), 119–131.
- Zemlyanova, A. Y., & Mogilevskaya, S. G. (2018). Circular inhomogeneity with Steigmann-Ogden interface: Local fields, neutrality, and Maxwell's type approximation formula. *International Journal of Solids and Structures*, 135, 85–98.